THE JOURNAL OF BIOLOGICAL CHEMISTRY VOL. 285, NO. 8, pp. 5497–5508, February 19, 2010

CHM-1, a New Vascular Targeting Agent, Induces Apoptosis of Human Umbilical Vein Endothelial Cells via p53-mediated Death Receptor 5 Up-regulation*[S]

Received for publication, June 30, 2009, and in revised form, November 22, 2009 Published, JBC Papers in Press, December 11, 2009, DOI 10.1074/jbc.M109.036277

An-Chi Tsai[‡], Shiow-Lin Pan[‡§1,2], Hui-Lung Sun[‡], Chih-Ya Wang[‡], Chieh-Yu Peng[‡], Shih-Wei Wang[‡], Ya-Ling Chang[‡], Sheng-Chu Kuo[¶], Kuo-Hsiung Lee[‖], and Che-Ming Teng[‡1,3]

From the [‡]Pharmacological Institute, College of Medicine, National Taiwan University, Taipei 10051, Taiwan, the [§]Graduate Institute of Pharmacology, Taipei Medical University, Taipei 10051, Taiwan, the [¶]Graduate Institute of Pharmaceutical Chemistry, China Medical University, Taichung 40402, Taiwan, and the [‖]Division of Medicinal Chemistry and Natural Products, School of Pharmacy, University of North Carolina, Chapel Hill, North Carolina 27599

CHM-1 (2′-fluoro-6,7-methylenedioxy-2-phenyl-4-quinolone) has been identified as a potent antitumor agent in human hepatocellular carcinoma; however, its role in tumor angiogenesis is unclear. This study investigated the effects of CHM-1 and the mechanisms by which it exerts its antiangiogenic and vascular disrupting properties. Using a xenograft model antitumor assay, we found that CHM-1 significantly inhibits tumor growth and microvessel formation. Flow cytometry, immunofluorescence microscopy, and cell death enzyme-linked immunosorbent assay kit revealed that CHM-1 inhibits growth of human umbilical vein endothelial cells (HUVEC) by induction of apoptotic cell death in a concentration-dependent manner. CHM-1 also suppresses HUVEC migration and capillary-like tube formation. We were able to correlate CHM-1-induced apoptosis in HUVEC with the cleavage of procaspase-3, -7, and -8, as well as with the cleavage of poly(ADP-ribose) polymerase by Western blotting assay. Such sensitization was achieved through up-regulation of death receptor 5 (DR5) but not DR4 or Fas. CHM-1 was also capable of increasing the expression level of p53, and most importantly, the induction of DR5 by CHM-1 was abolished by p53 small interfering RNA. Taken together, the results of this study indicate that CHM-1 exhibits vascular targeting activity associated with the induction of DR5-mediated endothelial cell apoptosis through p53 up-regulation, which suggests its potential as an antivascular and antitumor therapeutic agent.

In neoplasm, malignant angiogenesis and tumor mortality are highly associated with each other. Almost every step of aggressive tumor growth and metastatic dissemination relies on a functional vascular network to provide tumor cells with oxygen and nutrients and to remove waste products associated with tumor metabolism, a crucial hallmark of cancer (1). Nowadays, several antiangiogenic strategies have been developed to inhibit tumor growth and metastasis. In addition to the indirect interference of proangiogenic communication between the tumor and endothelial cell compartments, several recent reports have suggested that the induction of apoptosis in proliferation of endothelial cells may represent a potential therapeutic strategy in the treatment of neovascularization-related diseases (2–4). For instance, numerous natural angiogenic inhibitors, such as endostatin, angiostatin, and thrombospondin-1, act in part through selective triggering apoptosis in endothelial cells, resulting in vascular regression (5, 6). Several antitubulin-binding agents (*e.g.* CA-4-phosphate, ZD6126, and TZT-1027) and flavonoids (5,6-dimethylxanthenone-4-acetic acid) have demonstrated the ability to induce apoptosis of tumor vascular endothelial cells, leading to the rapid collapse and obstruction of tumor vessels and ultimately causing a tumor vascular shutdown effect (7).

Apoptosis is an intracellular suicide program possessing morphologic characteristics and biochemical features, including chromatin condensation, nuclear DNA fragmentation, cell shrinkage, membrane blebbing, and the formation of apoptotic bodies (8, 9). To date, two major apoptotic pathways have been described as follows: the extrinsic death receptor-mediated pathway and the intrinsic mitochondrion-initiated pathway. An apoptotic event engages the intrinsic mitochondrion-dependent processes, affecting mitochondrial permeability and resulting in cytochrome *c* release and activation of caspase-9. The extrinsic apoptotic pathway originates at membrane death receptors (DRs)[4] such as Fas (CD95/APO-1), DR4 (TRAIL-R1), and DR5 (TRAIL-R2) and then engages the intracellular apoptotic machinery involving adaptor molecules and proximal caspase-8 as well as distal executioner caspases (10, 11).

* This work was supported by National Science Council of Taiwan Research Grants 96-2628-B002-109-MY3 and 96-2321-B-002-031-MY2.

[S] The on-line version of this article (available at http://www.jbc.org) contains supplemental Figs. S1–S3 .

[1] Both authors contributed equally to this work.

[2] To whom correspondence may be addressed: Pharmacological Institute, College of Medicine, National Taiwan University, No. 1, Sec. 1, Jen-Ai Rd., Taipei 10051, Taiwan. Tel.: 886-2-23123456 (Ext. 88310); Fax: 886-2-2322-1742; E-mail: psl0826@ms13.hinet.net.

[3] To whom correspondence may be addressed: Pharmacological Institute, College of Medicine, National Taiwan University, No. 1, Sec. 1, Jen-Ai Rd., Taipei 10051, Taiwan. Tel.: 886-2-23123456 (Ext. 88310); Fax: 886-2-2322-1742; E-mail: cmteng@ntu.edu.tw.

[4] The abbreviations used are: DR, death receptor; HUVEC, human umbilical vein endothelial cell; PARP, poly(ADP-ribose) polymerase; Z, benzyloxycarbonyl; fmk, fluoromethyl ketone; siRNA, small interfering RNA; RT, reverse transcription; MTT, 3-(4,5-dimethylthiazol-2-yl)-2,5-diphenyltetrazolium bromide; PBS, phosphate-buffered saline; ELISA, enzyme-linked immunosorbent assay; TRAIL, tumor necrosis factor-related apoptosis-inducing ligand.

p53-inducible proapoptotic genes trigger apoptosis through both DR and mitochondrial apoptotic pathways (12). DRs such as DR4, DR5, and Fas are increased by p53-dependent transcriptional activation (13). Interaction of tumor necrosis factor-related apoptosis-inducing ligand (TRAIL), a member of the tumor necrosis factor family of proteins, with DR4 and DR5 leads to recruitment of the adaptor protein FADD and initiator caspase-8 to the death-inducing signaling complex (14). This results in enzymatic activation of caspase-8, which in turn activates a downstream caspase cascade in the presence or absence of mitochondrial amplification machinery (15, 16).

The 2-phenyl-4-quinolones and related compounds, a series of synthetic quinolone derivatives, were found to inhibit tubulin polymerization and disrupt microtubule organization, and they act as antimitotic agents (17–21). It was reported that the 2-phenylpyrroloquinolin-4-ones have antitumor activity *in vitro* and *in vivo* (22). In our previous study, we had speculated that CHM-1, which was identified from a synthetic 6,7-substituted 2-phenyl-4-quinolone derivative, potently inhibits hepatocyte growth factor-induced cell invasion in the human hepatocellular carcinoma cell line, SK-Hep-1, and exhibits a novel antimitotic antitumor activity against human hepatocellular carcinoma both *in vitro* and *in vivo* (23, 24). Recently, it was reported that CHM-1 has anticancer activity in human osteogenic sarcoma U-2 OS cells (25). However, there have been no reports on the possible vascular targeting effect of CHM-1. In this study, we investigated the mechanism of apoptosis induction by CHM-1 in endothelial cells. Our results suggest that CHM-1 targets tumor microvasculature through p53-mediated DR5 up-regulation.

EXPERIMENTAL PROCEDURES

Reagents—CHM-1 was synthesized by Prof. S.-C. Kuo (Graduate Institute of Pharmaceutical Chemistry, School of Medicine, China Medical University). Propidium iodide and 3-(4,5-dimethylthiazol-2-yl)-2,5-diphenyltetrazolium bromide (MTT) were obtained from Sigma. 4′,6-Diamidino-2-phenylindole was purchased from Roche Diagnostics. Antibody to caspase-3 was purchased from Imgenex (San Diego). Antibodies against PARP and caspase-9 were purchased from Cell Signaling Technology (Beverly, MA). Antibodies to caspase-6, caspase-7, caspase-8, and p53 were purchased from BD Biosciences. Antibodies against DR4 and DR5 were purchased from Novus Biologicals Inc. (Littleton, CO). Z-VAD-fmk was from R & D Systems (Minneapolis, MN). p53 small interfering RNA (siRNA) was obtained from Invitrogen. DR5 siRNA was purchased from Santa Cruz Biotechnology (Santa Cruz, CA).

Cell Culture and RNA Interference Transfection—Human umbilical vein endothelial cells (HUVEC) were freshly isolated from human umbilical cords and cultured as described previously (26). The human colorectal cancer HT-29 cell line was grown in RPMI 1640 medium with 10% heat-inactivated fetal bovine serum and penicillin (100 units/ml)/streptomycin (100 μg/ml) (27). These cells were maintained at 37 °C in a humidified incubator with 5% CO_2 atmosphere. For the transfection procedure, cells were grown to 70% confluence in a culture dish, and p53 siRNA or DR5 siRNA was transfected using Lipofectamine 2000 (Invitrogen). Following transfection, cells were seeded and treated with CHM-1 and then analyzed using MTT assay, Western blot analysis, or RT-PCR.

In Vivo Matrigel Plug Assay—Matrigel™ basement membrane matrix (BD Biosciences) mixed with heparin (10 units/ml) and endothelial growth medium-2 (EGM2), with or without CHM-1, were injected subcutaneously in the midventral abdominal region of C57BL/6 mice and permitted to solidify. On day 7, Matrigel pellets were harvested, fixed with 4% formalin, embedded in paraffin, and subsequently processed for Masson's Trichrome staining. Hb was estimated by the Drabkin's method with Drabkin's reagent kit (Sigma) to quantify blood vessel formation.

HT-29 Xenograft Models—CHM-1-phosphate was dissolved completely in a vehicle mixture of DMSO/cremophor EL/saline. Male SCID (severe combined immunodeficiency) mice were implanted subcutaneously with 1×10^7 HT-29 human colon cancer cells per mouse. Mice bearing established tumors ($\sim$100 mm^3) were randomized into two groups, and the agent treatment was initiated. CHM-1-phosphate at a dose of 25 mg/kg was administered intravenously every day. Tumors were measured every 3–4 days with a caliper, and tumor volumes were calculated using the following formula: volume (V) = $lw^2/2$, with l being the length and the w being the width. Histological analysis was done on formalin-fixed, paraffin-embedded xenograft tissue samples. The primary antibody CD31 (Abcam, Cambridge, MA) was used in this study to permit determination of the blood vessels. The protocols of all animal experiments were accordance with institutional guidelines for animal welfare.

Cell Viability and Growth—Cell viability was determined by measuring the ability of cells to transform the yellow tetrazolium salt MTT into formazan crystal, a purple dye. Cells (5×10^3 cells per well) were seeded in 96-well culture plates overnight for attachment and then were incubated with or without CHM-1 at different concentrations for 24 and 48 h. After the incubation, 0.5 mg/ml MTT solution was added to each well, and the plates were incubated at 37 °C for an additional 4 h. The color intensity of the formazan solution, which reflects the cell growth condition, was measured at 550 nm using an ELISA reader.

Endothelial Cell Migration Assay—HUVEC were plated (in complete medium) in the upper layer of an 8-μm pore size transwell. Cells were allowed to adhere for 4 h at 37 °C and then replaced the 2% heat-inactivated fetal bovine serum/M199 medium, with or without CHM-1, for 8 h at 37 °C in a humidified atmosphere of 95% air, 5% CO_2. At the same time, 5% heat-inactivated fetal bovine serum/M199 medium was added in the lower chambers. At the end of treatment, condition medium was removed from both upper and lower layers of chambers, and the membranes were fixed and stained with crystal violet for 10 min and then rinsed in water. Cells remaining on the filter side of the upper chamber were cleaned by gently wiping with a cotton swab. As the membranes dried, the cells that had migrated to the underside of the filters were photographed with microscope. To quantify the cells that had migrated through the membrane pores, the filters were gently cut from the chamber, and the dye was eluted in a solution

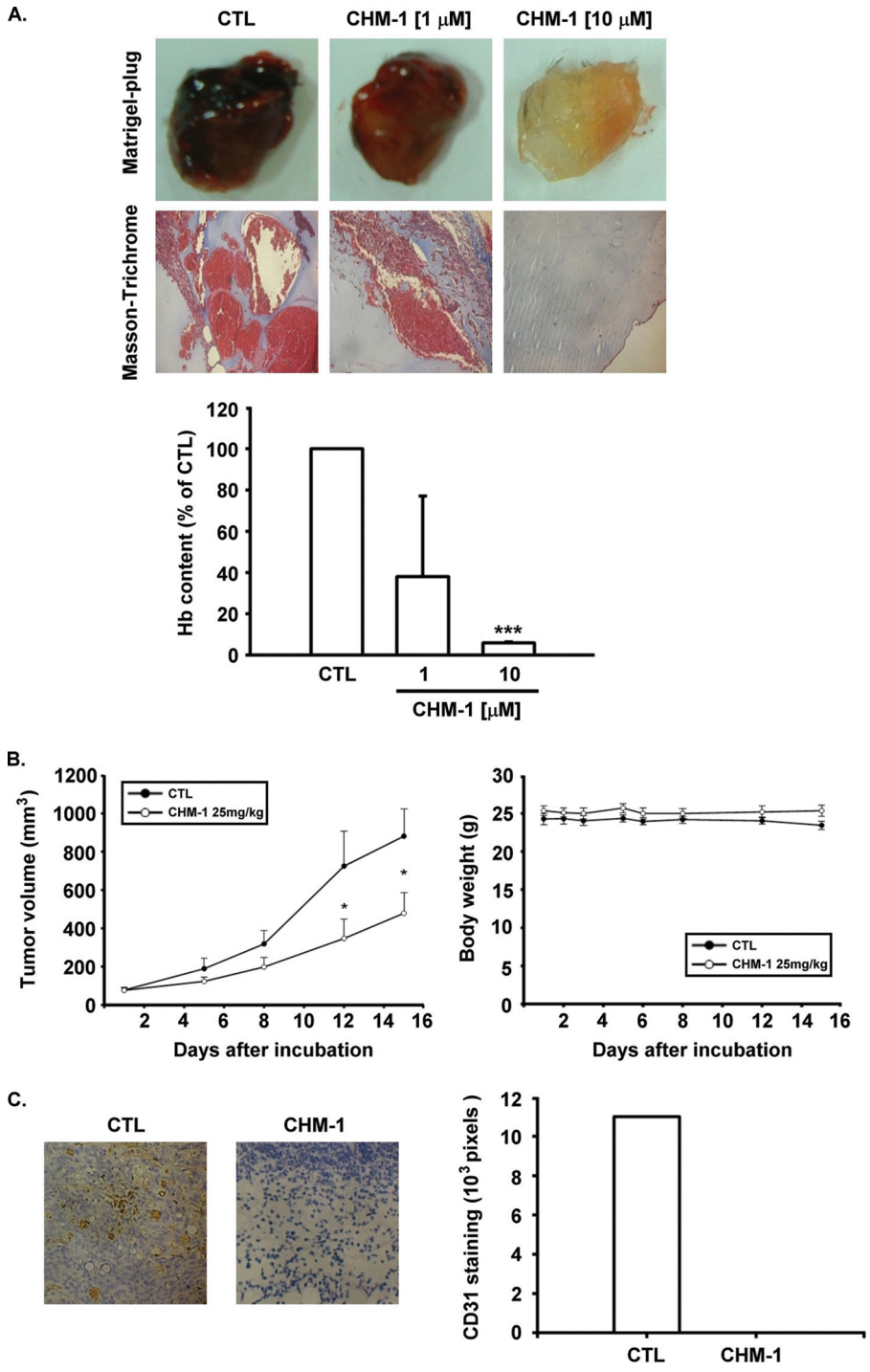

FIGURE 1. **Inhibitory effect of CHM-1 on *in vivo* angiogenesis.** *A,* Matrigel-plug bioassay for antiangiogenesis effect of CHM-1 in C57BL/6 mice. *Top panel,* representative macroscopic pictures of the Matrigel plugs after excision. *Middle panel,* histological sections of the Matrigel plugs stained with Masson's trichrome. *Bottom panel,* quantization of functional vasculature inside the Matrigel plugs by measuring Hb content using Drabkin's reagent. Data represent the mean ± S.E. from four independent experiments. ***, $p < 0.001$ as compared with the control (*CTL*) group. *B,* efficacy of CHM-1 on the growth of HT-29 human colon tumor xenografts and vascularization in SCID mice. Treatment with CHM-1 abrogated the tumor. *Left panel,* tumor growth is presented as the mean tumor volume (mm^3) ± S.E. Tumor volume was determined by caliper measurements and was calculated as the product of ½ × length × $width^2$. *Right panel,* body weight (g) of the mice. Each value represents the mean of at least seven animals. *, $p < 0.05$ as compared with the control (*CTL*) group. *C,* blood vessels of formalin-fixed paraffin-embedded sections from a xenograft tumor were detected by anti-CD31 immunofluorescence staining. *Brown color,* CD31-positive blood vessels. The images of vessel area in tumor sections stained with an antibody to CD31 were analyzed using an Image-Pro Plus software.

containing sodium citrate and then determined using an ELISA reader at A_{550}.

In Vitro Tube Formation Assay on Matrigel—3×10^4 HUVEC were incubated in the absence or presence of CHM-1 and then seeded in a 96-well culture plate precoated with Matrigel (BD Biosciences). The tubular formation was observed and photographed under a phase contrast microscope after incubation at 37 °C in a humidified chamber with 5% CO_2 for 6 h. The quantitative data were determined using Image analysis software (Image-Pro® Plus).

Evaluation of Apoptosis—Morphological analysis of cells apoptosis was examined by a phase contrast microscopy (Nikon). CHM-1-induced apoptotic death of HUVEC was identified by 4′,6-diamidino-2-phenylindole staining. Cells were seeded into 8-well slide chambers the day before treatment. After the cells were incubated with CHM-1 (3 μM) for 24 h, they were washed twice with ice-cold phosphate-buffered saline (PBS) and fixed in 4% methanol at −20 °C for 10 min. The cells were then incubated in 4′,6-diamidino-2-phenylindole for 5 min at room temperature. The slides were washed three times with PBS, and nuclear morphological alternations were then analyzed using a Zeiss fluorescence microscope. For quantitative assessment of oligonucleosomal DNA fragmentation, Cell Death ELISA^{PLUS} kit (Roche Diagnostics) was used to determined apoptosis. Spectrophotometric data at a wavelength of 405 nm, with a reference of 490 nm, was acquired on a microplate reader.

Flow Cytometric Analysis—The cells (80% confluence) were 2% fetal bovine serum/M199 medium-starved for 24 h to synchronize them in the G_0 phase of the cell cycle, and then they treated with CHM-1 for the indicated time. The cells were trypsinized after treatment, washed with cold PBS, and centrifuged. The pellet was fixed in 75% ethanol overnight at −20 °C. After centrifugation, the fixed cells

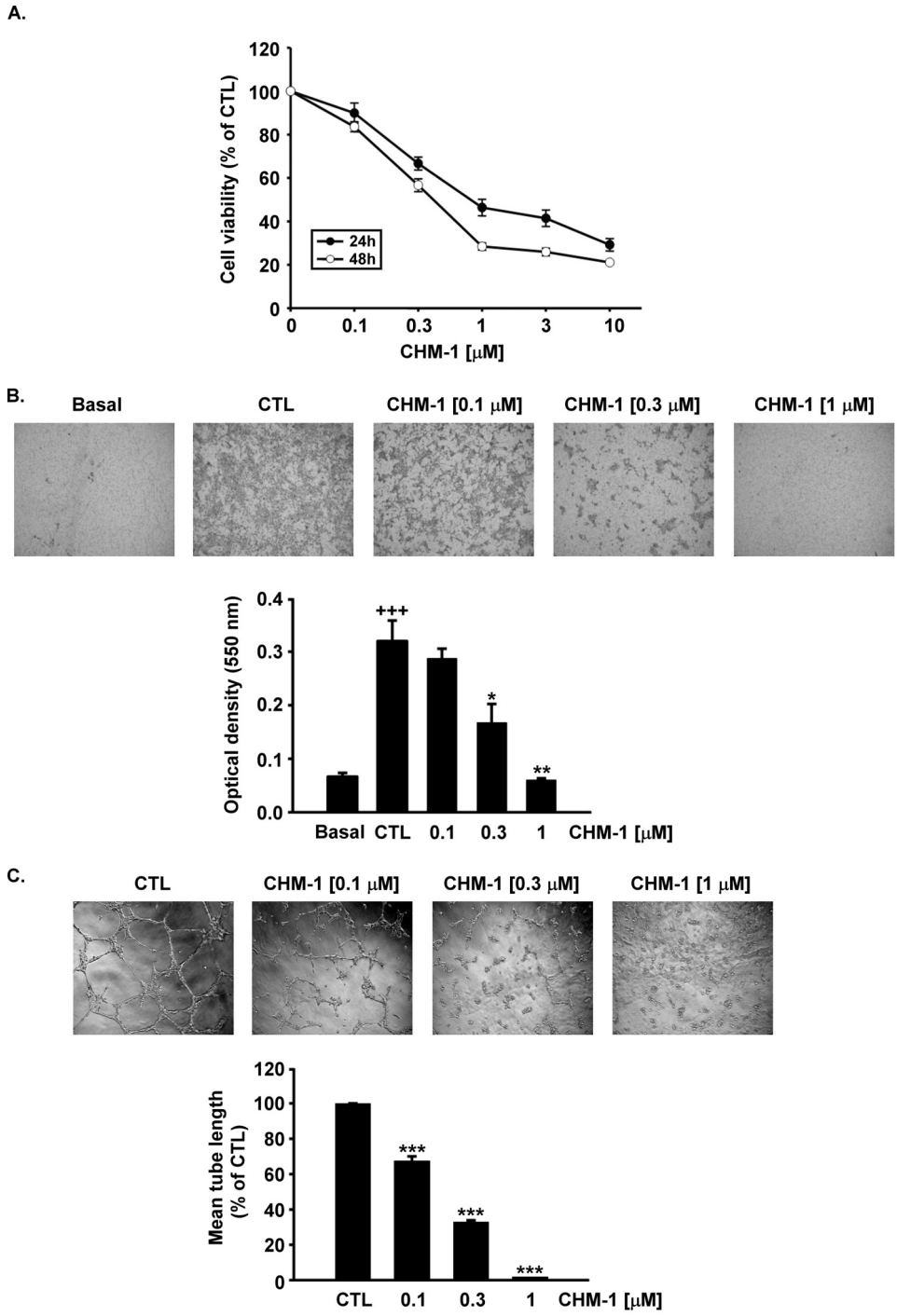

FIGURE 2. **Inhibitory effect of CHM-1 on *in vitro* angiogenesis.** *A,* cell viability (for 24 and 48 h) was determined using MTT reduction assay. *B,* inhibition of HUVEC migratory activity by CHM-1 was measured by a transwell migration assay. *Upper panel,* microscopic appearance of the migratory cells on the underside of the 8-μm pore size transwell membrane. *Lower panel,* quantitative data regarding endothelial cell migration. Data represent the mean ± S.E. from four independent experiments. +++, $p < 0.001$ as compared with the basal group; *, $p < 0.05$; **, $p < 0.01$ as compared with the control (*CTL*) group. *C, in vitro* Matrigel-based tubule formation assay. *Upper panel,* inhibitory effect of CHM-1 on the formation of endothelial cells capillary-like tubular structures as observed with a microscope. Magnification is ×100. *Lower panel,* quantification of the average tubular length was determined by image analysis software. Data represent the mean ± S.E. from four independent experiments. ***, $p < 0.001$ as compared with the control (*CTL*) group.

were washed once with PBS and incubated in 0.1 mol/liter phosphate/citric acid buffer (0.2 mol/liter Na_2HPO_4, 0.1 mol/liter citric acid, pH 7.8) for 30 min at room temperature in darkness. The cells were then centrifuged and resuspended with 0.5 ml of propidium iodide working solution (100 μg/ml RNase, 80 μg/ml propidium iodide, 0.1% Triton X-100 in PBS). The stained cells were sorted by FACScan flow cytometry and analyzed using CellQuest software (BD Biosciences).

Preparation of Cytosolic and Nuclear Extracts—For nuclear extracts, treated cells were washed with ice-cold PBS, scraped into buffer A (10 mM Hepes, pH 7.9, 1.5 mM $MgCl_2$, 10 mM KCl, 0.5 mM dithiothreitol, 1% Nonidet P-40, and protease inhibitors), and incubated on ice for 15 min. Nuclei were separated from the cytosol by centrifugation at 2,500 rpm for 5 min at 4 °C. The supernatants (cytosolic fraction) were removed, and the pellets were suspended in buffer C (20 mM Hepes, pH 7.9, 25% glycerol, 420 mM NaCl, 1.5 mM $MgCl_2$, 0.2 mM EDTA, 0.5 mM dithiothreitol, and 0.2 mM phenylmethylsulfonyl fluoride), incubated on ice for 30 min, and then centrifuged at 13,000 rpm for 10 min at 4 °C, and the supernatants were frozen at −20 °C.

Western Blot Analysis—The cells were harvested and lysed in an ice-cold modified RIPA buffer (150 mM NaCl, 1 mM EDTA, 1% Nonidet P-40, 0.5% sodium deoxycholate, 0.1% SDS, 20 mM Tris, pH 8.0) that was supplemented with protease inhibitors (1 μg/ml aprotinin, 1 μg/ml leupeptin, 0.5 M NaF, 0.5 M Na_3VO_4, 1 mM phenylmethylsulfonyl fluoride) for 1 h on ice. Cellular lysates were centrifuged at 13,000 rpm for 30 min at 4 °C to remove insoluble material. The protein concentration was determined by the Bio-Rad protein assay according to the manufacturer's instructions. Equal amounts of protein were separated on SDS-polyacrylamide gel electrophoresis gels, and the protein was subsequently transferred to nitrocellulose membranes by electroblotting 2.5 h at 400 mA. The membranes were blocked with 5% nonfat milk in PBS for 1 h and washed three times with PBS, 0.1% Tween 20. After that, the membranes were probed for desired proteins using specific primary antibodies overnight at 4 °C. Membranes were then washed four times with PBS, 0.1%

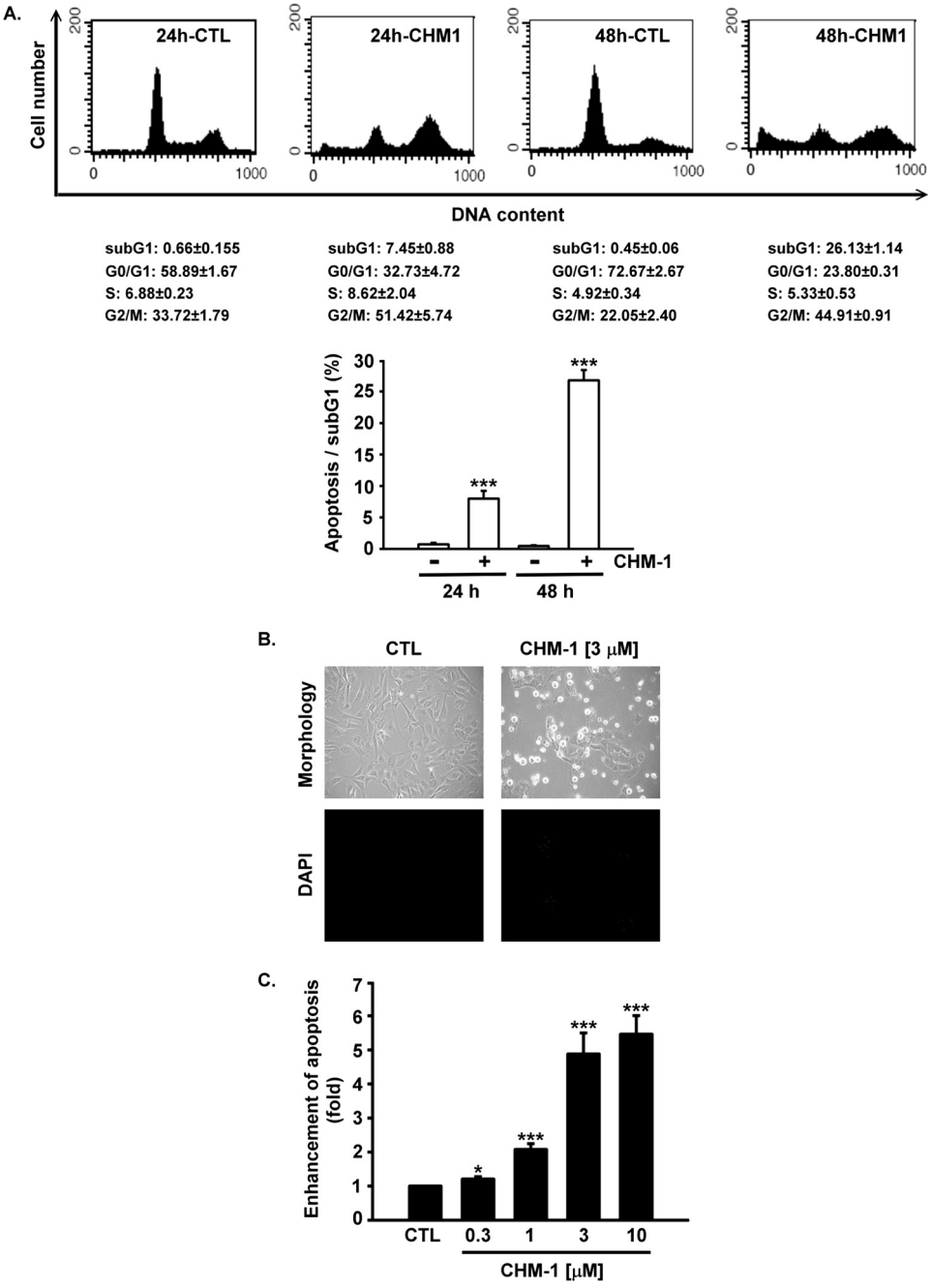

FIGURE 3. **CHM-1 triggers growth inhibition and apoptosis in HUVEC.** *A,* cells were treated with 3 μM CHM-1 for the indicated times. The appearance of a sub-G_1 population was analyzed by FACScan flow cytometric analysis. Data represent the mean ± S.E. from four independent experiments. ***, $p < 0.001$ as compared with the control group. *B, upper panel* displays the characteristic morphological features of apoptosis in cells after 24 h of treatment. In a parallel experiment, the cells were stained with 4′,6-diamidino-2-phenylindole (*DAPI*) solution. Stained nuclei were then observed under a fluorescent microscope. *C,* quantitative analysis of apoptotic cell death after 24 h of CHM-1 treatment. The amount of DNA fragmentation, a hallmark of apoptosis, was evaluated with a cell death ELISA^{PLUS} kit.

Tween 20 followed by peroxidase-conjugated appropriate secondary antibody and visualized by ECL detection system.

RT-PCR—Total cellular RNA was extracted from HUVEC with TRIzol reagent (Invitrogen). First strand cDNA synthesis was performed with 5 μg of RNA and 500 ng/μl random primers at 65 °C for 5 min and then using Moloney murine leukemia virus-RT at 37 °C for 1 h. The single-stranded cDNA was amplified by PCR. The amplification mixture (final volume, 20 μl) contained 10× *Taq* DNA polymerase buffer, 10 mM dNTPs, 10 μM primer pair, 0.5 μl of *Taq* DNA polymerase, cDNA, and diethyl pyrocarbonate water. The primers and PCR conditions used for DR5 were according to Cao *et al.* (28). PCR products were separated by 1.5% agarose gel electrophoresis and detected by ethidium bromide staining.

Statistical Analysis—Data are expressed as the mean ± S.E. for the indicated number of separate experiments. Means were checked for statistical difference using the *t* test, and *p* values less than 0.05 were considered significant. (*, $p < 0.05$; **, $p < 0.01$; and ***, $p < 0.001$). The significance of differences of *in vivo* xenograft data were analyzed by the Mann-Whitney *U* test.

RESULTS

CHM-1 Inhibits Angiogenesis in Vivo—To determine whether CHM-1 has antiangiogenic activities, an *in vivo* mouse Matrigel plug assay was first carried out. Angiogenesis was induced in EGM2-treated Matrigel plugs (control). However, CHM-1 potently inhibited EGM2-induced blood vessel growth in a concentration-dependent manner (Fig. 1*A*, *top panel*). We performed a histological examination to confirm the formation of numerous blood vessels. The stained section of the Matrigel plugs in the control groups showed abundant erythrocyte-filled vessels, indicating the formation of a functional vasculature in the Matrigel, whereas it was not observed in the CHM-1-treated plugs (Fig. 1*A*, *middle panel*). We also measured the hemoglobin content to quantify the antiangiogenic effect induced by the treatment with CHM-1. The hemoglobin quantity was markedly reduced by treatment with CHM-1 as compared with the control groups (Fig. 1*A*, *bottom panel*). To test the hypothesis that CHM-1 may disrupt vasculature within tumors, an HT-29 tumor xenograft model in SCID mice was used. CHM-1 treatment significantly inhibited tumor growth, without a toxic effect on body weight (Fig. 1*B*, *left* and *right panel*). We also performed immunohistochemical analysis of tissue samples with $CD31^+$ antibody, which is a specific endothelial marker for estimating whether CHM-1 sup-

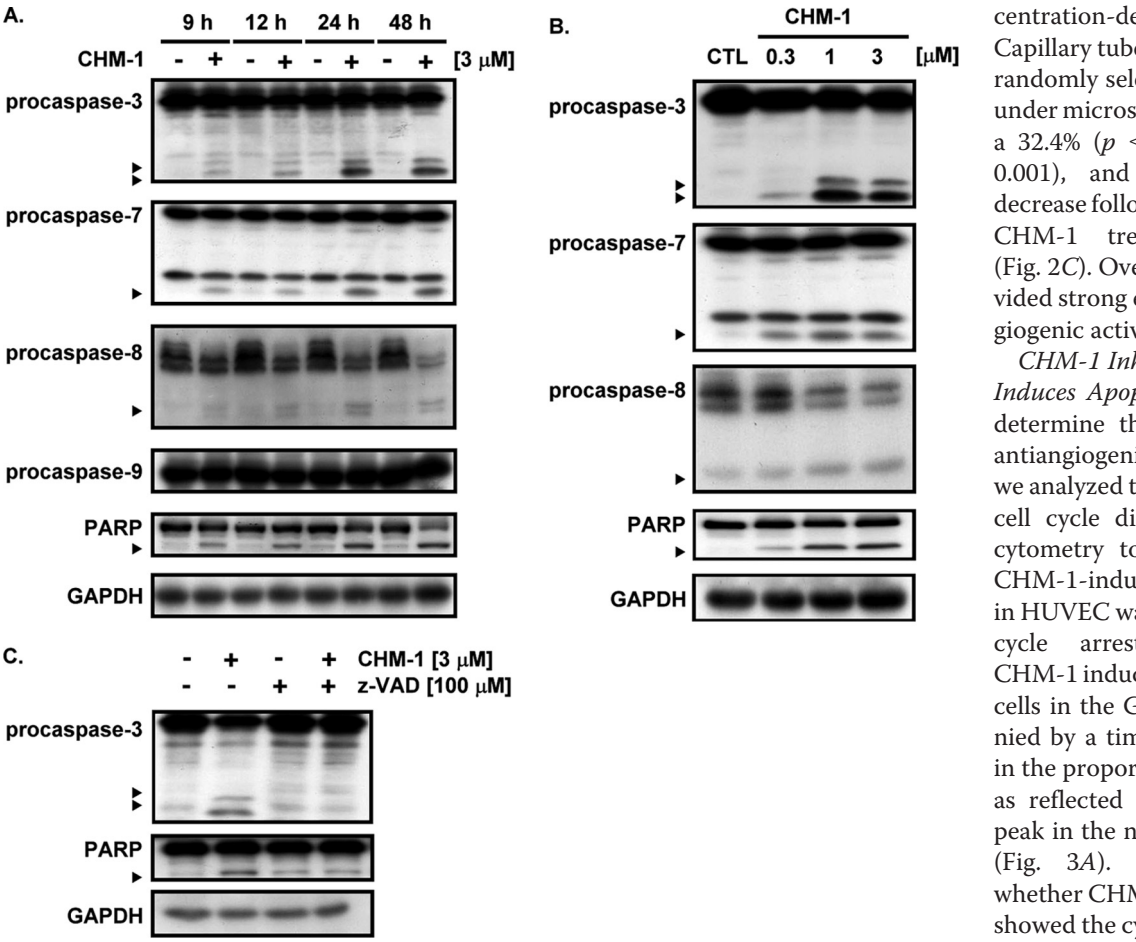

FIGURE 4. **CHM-1 induces proteolytic cleavage of caspases and PARP in HUVEC.** Cells were incubated in the absence or presence of CHM-1 for the indicated time (*A*) or concentration (*B*) and then harvested and prepared for detection of caspase-3, -7, -8, and -9 and PARP cleavage using Western blotting. *C,* pretreatment with Z-VAD-fmk for 1 h and then incubation with CHM-1 for another 24 h. Cells lysates were collected for Western blotting to detect the cleavage of caspase-3 and PARP. The *arrowheads* indicate cleavage forms. *GAPDH*, glyceraldehyde-3-phosphate dehydrogenase; *CTL*, control.

presses vasculature within tumors. In the treated group, vessels were sparsely distributed throughout the tumor, as evidenced by the lack of $CD31^+$ staining (Fig. 1*C*). Taken together, these results demonstrated antitumor activity of CHM-1 *in vivo* through the disruption of tumor microvasculature.

CHM-1 Inhibits Angiogenesis in Vitro—To assess the vascular targeting potential of CHM-1, we carried out an angiogenic cellular functional assay using HUVEC. We first executed an MTT assay to measure the effect of CHM-1 on the growth of HUVEC. The addition of CHM-1 resulted in time- and concentration-dependent cell growth inhibition, with IC_{50} values of 3.9 μM (24 h) and 1.1 μM (48 h), respectively (Fig. 2*A*). To examine whether CHM-1 affected the migratory behavior of endothelial cells, we performed a transwell migration assay. As illustrated in Fig. 2*B*, CHM-1 inhibited cell migration in a concentration-dependent manner. We proceeded to conduct a tube formation assay to estimate the effect of CHM-1 on morphological differentiation of the HUVEC. HUVEC were placed on a Matrigel-coated plate where they formed many strong, robust elongated tube-like structures in the presence of EGM2 (control). In contrast, treatment with CHM-1 strongly inhibited the formation of tube-like networks in a concentration-dependent manner. Capillary tubes were counted in five randomly selected areas of samples under microscopic field and showed a 32.4% ($p < 0.001$), 67.1% ($p < 0.001$), and 98% ($p < 0.001$) decrease following 0.1, 0.3, and 1 μM CHM-1 treatment, respectively (Fig. 2*C*). Overall, these results provided strong evidence of the antiangiogenic activity of CHM-1 *in vitro*.

CHM-1 Inhibits Cell Growth and Induces Apoptosis in HUVEC—To determine the mechanism of the antiangiogenic activity of CHM-1, we analyzed the effect of CHM-1 on cell cycle distribution using flow cytometry to investigate whether CHM-1-induced growth inhibition in HUVEC was accompanied by cell cycle arrest. Treatment with CHM-1 induced an accumulation of cells in the G_2/M phase, accompanied by a time-dependent increase in the proportion of apoptotic cells, as reflected by the presence of a peak in the number of sub-G_1 cells (Fig. 3*A*). We next examined whether CHM-1-induced cell death showed the cytological features that are typically seen in cells undergoing apoptosis. As shown in Fig. 3*B*, CHM-1 induced morphological changes and chromatin condensation, whereas untreated control cells displayed intact morphology and nuclear structure. Quantitative assessment of oligonucleosomal DNA fragmentation showed that CHM-1-treated cells increased this feature in a concentration-dependent manner (Fig. 3*C*). Overall, these results suggested that CHM-1 causes apoptosis in HUVEC.

CHM-1 Triggers the Extrinsic Apoptosis Pathway—The induction of CHM-1-induced apoptosis was additionally confirmed by the cleavage of PARP, which serves as a reliable biochemical marker of cells undergoing apoptosis. A decrease in total PARP with a concomitant increase in PARP cleavage fragments was observed in CHM-1-treated cells in a time- and concentration-dependent manner (Fig. 4, *A* and *B*). We further documented the involvement of various caspases during CHM-1-triggered cell death. Treatment with CHM-1 resulted in the induction of cleaved forms of caspase-3, -7, and -8, but not -9 (Fig. 4, *A* and *B*), indicating activation of the extrinsic apoptotic pathway. Pretreatment with the pan-caspase inhibitor Z-VAD-fmk was shown to reverse CHM-1-induced caspase-3 and PARP cleavage (Fig. 4*C*).

CHM-1 Induces Apoptosis via Up-regulation of DR5—Because CHM-1 induced the cleavage of initiator caspase-8, we speculated that its proapoptotic response could be mediated via

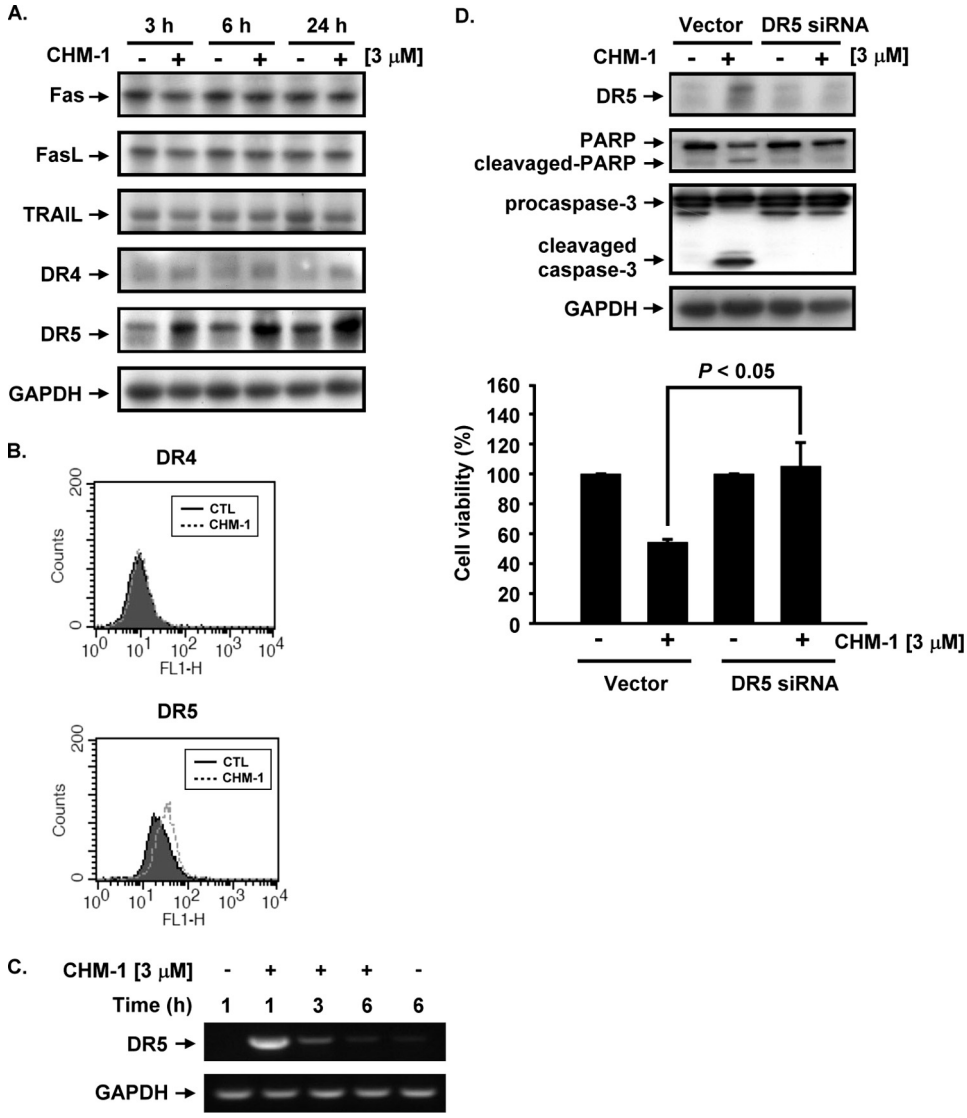

FIGURE 5. **CHM-1-induced apoptosis by up-regulation of DR5.** *A,* cells were exposed to CHM-1 (3 μM) for the indicated times and then harvested. Cell extracts were then prepared, followed by immunoblotting using antibodies against DRs (anti-Fas, anti-DR4, and anti-DR5) and ligands (anti-FasL and anti-TRAIL). *B,* HUVEC were incubated with CHM-1 (3 μM) for 24 h, and the levels of DR4/DR5 expression were analyzed by flow cytometry. *C,* HUVEC were treated with CHM-1 (3 μM) for the indicated times, and the expression of DR5 mRNA was then measured by RT-PCR analysis. *D,* knockdown of DR5 by DR5 siRNA attenuates CHM-1-induced apoptosis. HUVEC were transfected with or without DR5 siRNA and then incubated with or without CHM-1 (3 μM) for an additional 24 h. *Upper panel,* total cellular lysates were subjected to Western blot analysis of DR5, PARP, and caspase-3. *Lower panel,* cell viability was analyzed by crystal violet assay and is represented as the percentage (%) survival by setting untreated cells as 100%. *GAPDH,* glyceraldehyde-3-phosphate dehydrogenase.

the death receptor-signaling pathway. As shown in Fig. 5*A*, CHM-1 treatment was found to cause a time-dependent up-regulation of the DR5 protein without significant change in the expressions of FasL, TRAIL, Fas, and DR4. To confirm the effect of CHM-1 on DR5, we further measured the DR5 expression level at the cell surface using flow cytometry. CHM-1 consistently elevated the cell surface expression of DR5 but not DR4 in HUVEC (Fig. 5*B*). On the other hand, we also found that CHM-1 induced mRNA expression of DR5, reaching a maximum level at 1 h (Fig. 5*C*). To further evaluate the role of DR5 in CHM-1-induced apoptotic signaling in HUVEC, we used DR5 siRNA to block CHM-1-induced DR5 up-regulation and then determined its effect on CHM-1-induced apoptosis. The prevention of PARP and caspase-3 cleavage due to CHM-1 treatment was correlated with the decrease in DR5 protein levels by the transfection of DR5 siRNA (Fig. 5*D*, *upper panel*). Using the crystal violet assay, we also found that CHM-1-induced growth inhibition in HUVEC was nearly suppressed by DR5 siRNA (Fig. 5*D*, *lower panel*). Taken together, these results suggested that DR5 up-regulation plays an important role in CHM-1-induced apoptosis in HUVEC.

Up-regulation of DR5 by CHM-1 Correlates with the Increased Expression of p53—In a previous study, we found a great deal of evidence indicating that p53, a transcriptional factor, could activate the extrinsic DR pathway through the induction of genes encoding transmembrane proteins such as DR5 (12). Therefore, we first determined whether CHM-1 up-regulated the expression of p53, thereby regulating the expression of DR5 in HUVEC. As shown in Fig. 6*A*, treatment with CHM-1 increased the p53 protein level and translocated p53 into the nucleus, which is coincident with the change in DR5 protein level. Next, to elucidate whether p53 plays a critical role in CHM-1-induced DR5 up-regulation and apoptosis, we manipulated p53 expression using p53 siRNA. The data showed that knockdown of p53 attenuated the induction of DR5 as well as the cleavage of PARP and caspase-3 (Fig. 6*B*) and consequently prevented growth inhibition and apoptosis in cells treated with CHM-1 (Fig. 6*C*).

DISCUSSION

In our previous study, CHM-1 was shown to possess potent cytotoxic activity *in vitro* and *in vivo*. CHM-1 was found to bind to tubulin at the colchicine site, causing G_2/M phase cell arrest and inducing cancer cell apoptosis (24). Recently, several studies have consistently reported that some microtubule-targeting agents, particularly those agents that work by acting at the colchicine-binding site of the β-subunit of endothelial tubulin, may disrupt the endothelial cytoskeleton, leading to loss of blood flow and tumor-related endothelial cell apoptosis and eventually tumor vasculature disruption (29, 30). In this study, we first demonstrated that CHM-1 suppressed tumor growth

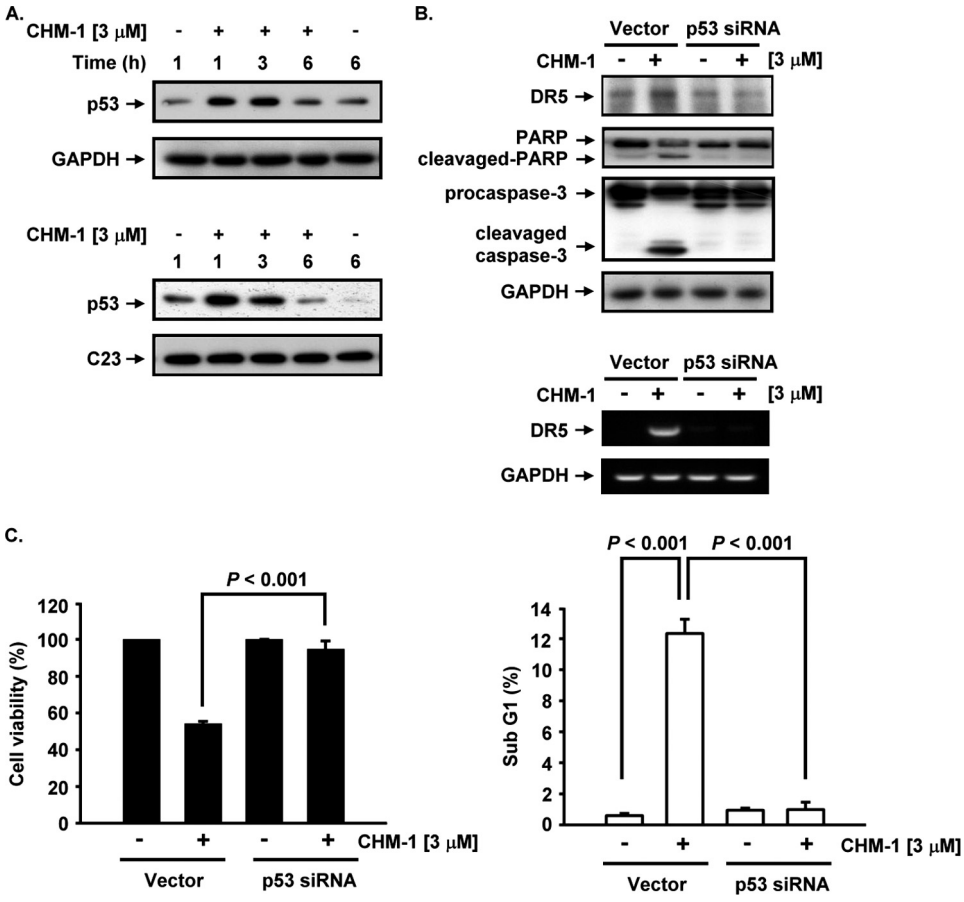

FIGURE 6. **Contribution of p53 to CHM-1-induced apoptosis in HUVEC.** *A,* CHM-1-induced p53 expression in HUVEC. Treatment with CHM-1 (3 μM) for the indicated times, either total cellular (*upper panel*) or nuclear lysates (*lower panel*), was subjected to Western blot analysis using antibody specific for p53. *B,* inhibition of p53 activation contributed to the down-regulation of DR5 in CHM-1-treated cells. HUVEC were pretreated with or without p53 siRNA for 48 h and then incubated with or without CHM-1 (3 μM) for 24 h. *Upper panel,* total cellular lysates were subjected to Western blot analysis of DR5, PARP, and caspase-3. *Lower panel,* expression of DR5 mRNA was demonstrated by RT-PCR. *C,* control or DR5 siRNA-transfected HUVEC were treated with CHM-1 (3 μM) for 24 h. *Left panel,* cell viability was measured by crystal violet assay and expressed as a percentage of the untreated control. *Right panel,* cells stained with propidium iodide and the percentage of cells in the sub-G_1 phase (reminiscent of apoptotic cells) were estimated by FACScan flow cytometric analysis. *GAPDH*, glyceraldehyde-3-phosphate dehydrogenase.

through induction of endothelial cell apoptosis, which disrupted tumor microvascular networks.

We provided strong evidence that CHM-1 significantly inhibits tumor angiogenesis using Matrigel-plug and xenograft animal models. We then showed that CHM-1 blocked endothelial cell functions such as cell survival, migration, and tube formation, in agreement with our *in vivo* findings. The previous study demonstrates that CHM-1 significantly inhibits the migration of U-2 OS cell migration at 3 μM (25); however, the inhibition of endothelial cell migration by CHM-1 was observed with lower concentration (0.1–1 μM). We also found that the microtubule polymerization of HUVEC was disrupted by CHM-1 (supplemental Fig. S1). Based on these results, we conclude that CHM-1 may be a novel vascular targeting agent for cancer treatment.

The mechanisms of vascular target therapies include preventing the formation of new blood vessels or revascularization and/or disrupting the existing vasculature of a tumor. Endothelial cell apoptosis plays a pivotal role in the sculpting of blood vessels (31). It has been reported that the induction of endothelial cell apoptosis may represent a common feature among antiangiogenic molecules (6, 32). Accumulating evidence suggests that many cytotoxic agents and antiangiogenic inhibitors act via the induction of endothelial cell apoptosis to suppress endothelial cell proliferation or migration and then to restrict tumor progression (33, 34). In this study, we found accumulation of cells at the G_2/M phase in CHM-1-treated cells. We also measured the effect of CHM-1 on the cell cycle regulatory proteins. The results of this study show that CHM-1 did not alter the level of Cdc2 expression, but it did cause a dramatic increase of MPM2, cyclin B1 protein expression, and Cdc25C phosphorylation. Moreover, Tyr-15-phosphorylated Cdc2 expression was decreased and Thr-161-phosphorylated Cdc2 expression was increased after CHM-1 treatment at the indicated times (supplemental Fig. S2). These results are similar with those reported by Wang *et al.* (24). The results of flow cytometric analysis were also shown at an elevated sub-G_1 peak in CHM-1-treated cells, reflecting the effect of apoptosis. We confirmed this by detecting apoptotic morphological and biochemical features of the cells. These data suggest that CHM-1 might induce apoptosis in proliferating endothelial cells.

Caspases play a critical role in apoptosis and in development. Recent evidence indicates two major types of signaling pathways in activated caspase-8 amplify apoptotic signals as follows: one directly cleaves and activates downstream effector caspases such as caspase-3/7, and the second activates the intrinsic apoptotic pathway by processing Bid, which is an intracellular molecule that bridges the apoptotic interaction between the membrane DRs and the mitochondria. The cleaved Bid is then translocated into the mitochondria, and through subsequent interaction with pro-apoptotic Bax, the mitochondria-dependent apoptotic pathway is stimulated, thereby activating caspase-3/7 (35, 36). However, our previous study demonstrates that neither initiator nor effector caspases participate in CHM-1-mediated apoptosis in human hepatocellular carcinoma cells. CHM-1 appears to induce apoptotic cell death via the caspase-independent pathway (24). The results of this study show that proteolytic procaspase-8, -3, and -7 are cleaved but procaspase-9 is not. Caspase-3 processing and subsequent PARP cleavage can be prevented by addition of the caspase inhibitor Z-VAD-fmk (Fig. 4). Furthermore, treatment with

CHM-1 in HUVEC does not induce the cleavage of protein Bid (supplemental Fig. S3). These results indicate that CHM-1 triggers apoptosis in HUVEC by the extrinsic caspase-dependent pathway.

Within the extrinsic apoptotic pathway, caspase-8 is the most proximal caspase that transmits apoptotic signals originating at the membrane DRs (36). We reasoned that if CHM-1 results in activation of caspase-8, it should be through the up-regulation of DRs in HUVEC. The data indicate that CHM-1 increased the expression of DR5, but not DR4 and Fas, and that the effects were manifested not only in protein levels but also in the cell surface fraction in HUVEC. On the other hand, TRAIL induces apoptosis by activating caspase-8 via its receptors DR4 and/or DR5 (16). HUVEC express both DR4 and DR5, and apoptosis is induced following treatment with TRAIL (37). Recent studies, however, indicate that DR levels can be enhanced by endogenous induction or exogenous overexpression. Several genotoxic and nongenotoxic agents can induce apoptosis by increasing endogenous DR5 (38). On the other hand, exogenously overexpressed DR5, without concomitant up-regulation in its ligand levels, has been shown to be associated with induction of apoptosis (39). In this study, our results demonstrated that CHM-1-induced apoptosis is coupled with DR5 induction without changes in the expression of its ligand, TRAIL. It is therefore possible that CHM-1 activated DR5 to induce cell death in a ligand-independent manner. The up-regulation of DR5 mRNA was also seen as early as 1 h after CHM-1 treatment and was coupled with similar changes at the protein level. Moreover, we found that DR5 siRNA efficiently prevented the expression of cleaved forms of caspase-3 and PARP and growth inhibition after CHM-1 treatment.

p53 is a major tumor suppressor protein that exerts its effects on multiple aspects of tumor formation. As a sensor of cellular stress, the p53 tumor suppressor protein is a well established critical apoptosis initiator that contributes to the cellular emergency-response mechanism (12). Previous evidence has demonstrated that p53 is involved in the paclitaxel (taxol)-induced growth arrest or apoptosis in HUVEC (40), adenovirus-mediated p53 transfer (41), pigment epithelial-derived factor (42), and 15-deoxy$^{\Delta 12,14}$-prostaglandin J_2 (43). These findings prompted us to investigate the involvement of p53 in CHM-1-induced HUVEC apoptosis. As shown in Fig. 6*A*, we found that treatment with CHM-1 induced the expression of p53 and its accumulation in the nucleus. Moreover, the concentration of CHM-1 required to increase p53 protein expression was the same as that needed to induce apoptosis. Thus, we suggest that p53 may be involved in CHM-1-triggered apoptosis in HUVEC. In response to various stress-associated signals, p53 stimulates a wide network of signals that act through two major apoptotic pathways, the extrinsic DR pathway or intrinsic mitochondrial pathway, and consequently triggers the activation of a caspase cascade. Furthermore, p53 exerts its apoptotic functions by transcriptionally activating an ever-increasing number of target genes that in turn lead directly or indirectly to cell death (12). Evidence indicates that p53 can activate the extrinsic DR pathway through the induction of genes encoding transmembrane proteins such as DR5 (39). We therefore examined whether the induction of DR5 expression by CHM-1 in HUVEC correlated with p53 status. The representative result shown in Fig. 6*B* indicates that knockdown of p53 by p53 siRNA can inhibit both protein and mRNA expression levels of DR5. These results suggest that CHM-1 induced the up-regulation of DR5 mediated by p53 induction. This study showed that p53 activation was critical for CHM-1-induced apoptosis, because knockdown of p53 blocked/inhibited CHM-1-mediated apoptosis. On the other hand, transfected p53 siRNA into HUVEC clearly suppressed CHM-1-induced cleavage of caspase-3 and PARP and dramatically reversed CHM-1-induced cell growth inhibition (Fig. 6, *B* and *C*). Overall, these results identify p53 as a crucial proapoptotic protein in apoptosis induced by CHM-1 in HUVEC.

In conclusion, our study demonstrates that CHM-1 exhibits a potent antineovascularization effect *in vitro* and *in vivo*, interfering with several pivotal steps in the neovascularization process, including endothelial cells growth, migration, and differentiation (capillary tube formation). Our results also show that CHM-1 induces HUVEC apoptosis through up-regulation of p53 and subsequent induction of DR5-mediated extrinsic apoptotic signaling pathways. The ability to induce HUVEC apoptosis *in vivo* suggests that CHM-1 can prevent the formation of new blood vessels and can also eliminate existing vessels within tumors. These observations provide the pharmacological basis for developing CHM-1 for therapeutic application in pathological angiogenesis-related diseases such as cancer.

REFERENCES

1. Shchors, K., and Evan, G. (2007) *Cancer Res.* **67,** 7059–7061
2. Quesada, A. R., Muñoz-Chápuli, R., and Medina, M. A. (2006) *Med. Res. Rev.* **26,** 483–530
3. Cooney, M. M., van Heeckeren, W., Bhakta, S., Ortiz, J., and Remick, S. C. (2006) *Nat. Clin. Pract. Oncol.* **3,** 682–692
4. Heath, V. L., and Bicknell, R. (2009) *Nat. Rev. Clin. Oncol.* **6,** 395–404
5. Ribatti, D. (2009) *Leuk. Res.* **33,** 638–644
6. Dimmeler, S., and Zeiher, A. M. (2000) *Circ. Res.* **87,** 434–439
7. Lippert, J. W., 3rd (2007) *Bioorg. Med. Chem.* **15,** 605–615
8. Taatjes, D. J., Sobel, B. E., and Budd, R. C. (2008) *Histochem. Cell Biol.* **129,** 33–43
9. Taylor, R. C., Cullen, S. P., and Martin, S. J. (2008) *Nat. Rev. Mol. Cell Biol.* **9,** 231–241
10. Grütter, M. G. (2000) *Curr. Opin. Struct. Biol.* **10,** 649–655
11. Siegel, R. M., and Lenardo, M. J. (2002) *Current Protocols in Cytometry: Apoptosis Signaling Pathways*, NIAID, National Institutes of Health, Bethesda, MD
12. Haupt, S., Berger, M., Goldberg, Z., and Haupt, Y. (2003) *J. Cell Sci.* **116,** 4077–4085
13. Bates, S., and Vousden, K. H. (1999) *Cell. Mol. Life Sci.* **55,** 28–37
14. Tas, F., Duranyildiz, D., Soydinc, H. O., Cicin, I., Selam, M., Uygun, K., Disci, R., Yasasever, V., and Topuz, E. (2008) *Cancer Chemother. Pharmacol.* **61,** 721–725
15. MacFarlane, M. (2003) *Toxicol. Lett.* **139,** 89–97
16. Mahalingam, D., Szegezdi, E., Keane, M., Jong, S., and Samali, A. (2009) *Cancer Treat. Rev.* **35,** 280–288
17. Kuo, S. C., Lee, H. Z., Juang, J. P., Lin, Y. T., Wu, T. S., Chang, J. J., Lednicer, D., Paull, K. D., Lin, C. M., Hamel, E., *et al.* (1993) *J. Med. Chem.* **36,** 1146–1156
18. Li, L., Wang, H. K., Kuo, S. C., Wu, T. S., Lednicer, D., Lin, C. M., Hamel, E., and Lee, K. H. (1994) *J. Med. Chem.* **37,** 1126–1135
19. Xia, Y., Yang, Z. Y., Xia, P., Bastow, K. F., Tachibana, Y., Kuo, S. C., Hamel, E., Hackl, T., and Lee, K. H. (1998) *J. Med. Chem.* **41,** 1155–1162
20. Xia, Y., Yang, Z. Y., Xia, P., Hackl, T., Hamel, E., Mauger, A., Wu, J. H., and Lee, K. H. (2001) *J. Med. Chem.* **44,** 3932–3936

21. Chen, Y. C., Lu, P. H., Pan, S. L., Teng, C. M., Kuo, S. C., Lin, T. P., Ho, Y. F., Huang, Y. C., and Guh, J. H. (2007) *Biochem. Pharmacol.* **74,** 10–19
22. Ferlin, M. G., Chiarelotto, G., Gasparotto, V., Dalla Via, L., Pezzi, V., Barzon, L., Palù, G., and Castagliuolo, I. (2005) *J. Med. Chem.* **48,** 3417–3427
23. Wang, S. W., Pan, S. L., Peng, C. Y., Huang, D. Y., Tsai, A. C., Chang, Y. L., Guh, J. H., Kuo, S. C., Lee, K. H., and Teng, C. M. (2007) *Cancer Lett.* **257,** 87–96
24. Wang, S. W., Pan, S. L., Huang, Y. C., Guh, J. H., Chiang, P. C., Huang, D. Y., Kuo, S. C., Lee, K. H., and Teng, C. M. (2008) *Mol. Cancer Ther.* **7,** 350–360
25. Hsu, S. C., Yang, J. S., Kuo, C. L., Lo, C., Lin, J. P., Hsia, T. C., Lin, J. J., Lai, K. C., Kuo, H. M., Huang, L. J., Kuo, S. C., Wood, W. G., and Chung, J. G. (2009) *J. Orthop. Res.* **27,** 1637–1644
26. Peng, C. Y., Pan, S. L., Lee, K. H., Bastow, K. F., and Teng, C. M. (2008) *Cancer Lett.* **263,** 114–121
27. Chen, T. H., Pan, S. L., Guh, J. H., Liao, C. H., Huang, D. Y., Chen, C. C., and Teng, C. M. (2008) *Clin. Cancer Res.* **14,** 4250–4258
28. Cao, L., Li, Y., Cheng, F., Li, S., and Long, D. (2006) *Transplant. Proc.* **38,** 2207–2209
29. Meng, F., Cai, X., Duan, J., Matteucci, M. G., and Hart, C. P. (2008) *Cancer Chemother. Pharmacol.* **61,** 953–963
30. Schwartz, E. L. (2009) *Clin. Cancer Res.* **15,** 2594–2601
31. Duval, H., Harris, M., Li, J., Johnson, N., and Print, C. (2003) *Angiogenesis* **6,** 171–183
32. Sakamaki, K. (2004) *Curr. Neurovasc. Res.* **1,** 305–315
33. Folkman, J. (2003) *Semin. Cancer Biol.* **13,** 159–167
34. Tozer, G. M., Kanthou, C., and Baguley, B. C. (2005) *Nat. Rev. Cancer* **5,** 423–435
35. Kruidering, M., and Evan, G. I. (2000) *IUBMB Life* **50,** 85–90
36. Li, J., and Yuan, J. (2008) *Oncogene* **27,** 6194–6206
37. Li, J. H., Kirkiles-Smith, N. C., McNiff, J. M., and Pober, J. S. (2003) *J. Immunol.* **171,** 1526–1533
38. Sheikh, M. S., Burns, T. F., Huang, Y., Wu, G. S., Amundson, S., Brooks, K. S., Fornace, A. J., Jr., and el-Deiry, W. S. (1998) *Cancer Res.* **58,** 1593–1598
39. Wu, G. S., Kim, K., and el-Deiry, W. S. (2000) *Adv. Exp. Med. Biol.* **465,** 143–151
40. Pasquier, E., Carré, M., Pourroy, B., Camoin, L., Rebaï, O., Briand, C., and Braguer, D. (2004) *Mol. Cancer Ther.* **3,** 1301–1310
41. Teodoro, J. G., Parker, A. E., Zhu, X., and Green, M. R. (2006) *Science* **313,** 968–971
42. Ho, T. C., Chen, S. L., Yang, Y. C., Liao, C. L., Cheng, H. C., and Tsao, Y. P. (2007) *Cardiovasc. Res.* **76,** 213–223
43. Ho, T. C., Chen, S. L., Yang, Y. C., Chen, C. Y., Feng, F. P., Hsieh, J. W., Cheng, H. C., and Tsao, Y. P. (2008) *J. Biol. Chem.* **283,** 30273–30288